PAPER

Selective nano-emitter fabricated by silver assisted chemical etch-back for multicrystalline solar cells

Y. Wang,[ab] Y. P. Liu,*[ab] T. Lai,[c] H. L. Liang,[ab] Z. L. Li,[c] Z. X. Mei,*[ab] F. M. Zhang,[c] A. Kuznetsov[d] and X. L. Du[ab]

A nano-emitter is fabricated by one-step Ag-assisted chemical etch-back after conventional POCl$_3$ diffusion, with the intention of overcoming the relatively low efficiency of black silicon solar cells. The conversion efficiency of the multicrystalline silicon nano-emitter solar cell with a suitable sheet resistance is significantly improved thanks to the increased open-circuit voltage, short current and fill factor, all arising from the reduced surface recombination and Auger recombination, as well as the improved ohmic contact. In order to further improve the performance of the solar cell, it is combined with the selective emitter technique, resulting in a multicrystalline silicon selective nano-emitter solar cell. The selective emitters – etched back for different sheet resistances – are investigated to optimize the conversion efficiency. A 16.94% conversion efficiency is finally achieved with a sheet resistance of 107 Ω sq^{-1}, which is 0.34% higher than a standard selective emitter solar cell. Such an improved efficiency can be attributed to a lower reflectivity, a more homogeneous emitter, a smaller surface area and Auger recombination.

Introduction

Solar cells have drawn a lot of attention in recent decades because of the great need for clean and renewable energy. The majority of solar cells are silicon based, due to such cells' relatively low price and high efficiency. However, although many groups have done a lot of work to enhance the conversion efficiency, it still has not reached its theoretical efficiency limit. The reduced conversion efficiency is mainly attributed to optical losses and electrical losses. In this case, there are two common approaches to improve the efficiency of silicon solar cells. One fundamental solution is to increase the light harvest. Light trapping structures, such as pyramidal structures,[1] 'worm like' structures,[2] nanowires,[3] and porous Si,[4] are an effective way to reduce the reflectivity and obtain more incident light. On the other hand, decreasing the electrode contact area on the front side or employing a back contact is another potent method to reduce the shading losses and increase light absorption.[5] Basically, the more light harvested, the higher the efficiency that is achieved. Another approach that should be tried is to collect as many photo-generated carriers as possible – *i.e.* to reduce the recombina-

tion in the whole cell and improve the collection efficiency of the electrode.

To enhance the light absorption of silicon solar cells, black silicon is quite a good candidate. Black silicon, a surface modification of silicon with very low reflectivity and correspondingly high absorption of visible and infrared light, can be obtained by means of a needle-shaped surface structure,[6,7] nanowire structure,[3,8] porous surface,[4,9,10] and so on. It was first discovered in the 1980s as an unwanted side effect of reactive ion etching (RIE),[11] but later purposefully developed in Eric Mazur's laboratory by using femtosecond laser pulses.[6] After that, a lot of techniques, both physical and chemical, have been employed to fabricate black silicon, such as plasma technology,[12] electrochemical etching and metal-assisted chemical etching.[4,9,10,13,14] Metal-assisted chemical etching has been widely researched as a way to obtain black silicon solar cells, because of its low cost and simple process. As reported previously, we have used AgNO$_3$/HF solution to fabricate large-area black silicon on both crystalline silicon (c-Si) and multicrystalline silicon (mc-Si) by a one-step method. The average reflectivity was reduced to as low as 2% for c-Si and 4% for mc-silicon, from 300 to 1000 nm with no AR coating. However, even with a SiO$_2$, SiN$_x$ bilayer passivation process, the efficiency of the black mc-Si cell was only 15.8%. Such low efficiency was attributed to a deficient current passivation method and the formation of an excess dead layer on the nano-emitter (NE) surface during the P diffusion process, which greatly affects the blue response.[15] Very recently, Jihun Oh *et al.* also figured out that the nanostructure of metal-assisted etched black silicon worsened both the

[a]*Beijing National Laboratory for Condensed Matter Physics, Institute of Physics, Chinese Academy of Sciences, Beijing 100190, China.*
E-mail: zxmei@aphy.iphy.ac.cn; ypliu@aphy.iphy.ac.cn
[b]*Key Laboratory for Renewable Energy, Chinese Academy of Science, Beijing Key Laboratory for New Energy Materials and Devices, Beijing 100190, China*
[c]*Tianwei New Energy Holdings Co., Ltd, Chengdu 610200, China*
[d]*Department of Physics, University of Oslo, No-0316, Norway*

surface recombination and the Auger recombination channels by increasing the surface area and altering the doping profile, which results in low conversion efficiency, even with low reflection.[16] Accordingly, black silicon should have a balance between reflectivity and recombination.

The common sheet resistance for commercial silicon solar cell is about 40–60 Ω sq^{-1} with homogeneous doping in the emitter region in order to obtain a good ohmic contact at the metal-semiconductor interface. However, such a heavy doping concentration would increase the surface recombination velocity, and thus decrease the performance of cells.[17] To minimize the emitter recombination so as to improve the blue response of the silicon solar cell, a proper doping concentration at different areas is required. A trade-off compromise could be obtained by a selective emitter (SE) structure, in which only metal-contacted regions are heavily doped and the illuminated areas are lightly doped. SEs have been realized by various techniques including diffusion with barrier,[18] printing doping ink[19] and emitter etch-back.[20,21] However, the wet chemical etch-back method stands out from other methods because of its cost-effectiveness. The basic procedure of the wet chemical etch-back method begins with uniform texturization and heavy diffusion. The region on the emitter that will be the contact is then masked with an acid resistant material. Subsequently, the silicon wafer is etched back using the HF/HNO$_3$ system, which is followed by applying unaltered standard PECVD-SiN$_x$ coating, screen printing and co-firing after removal of the mask.

In this letter, we report the fabrication of a nano-emitter (NE) by one-step Ag-assisted chemical etching after conventional PN junction formation, in order to reduce the reflectivity, remove the dead layer and eliminate the increased Auger recombination during the POCl$_3$ diffusion. However, as the etching time and the size of the nanostructures increased, the sheet resistance was too high to achieve ohmic contact. Hence, the etch-back time of the NE should be short enough to guarantee the low sheet resistance for good contact. In this case, the advantage of a low reflectivity nano-emitter cannot be achieved efficiently. For further improvement, the nano-emitter was altered with a wet chemical etch-back SE technique, resulting in a selective nano-emitter (SNE). This SNE was achieved by employing HF/AgNO$_3$ as the etch-back solution instead of the HF/HNO$_3$ system. Hence, not only can the light harvest be increased, but the sheet resistance of the emitter can also be controlled precisely.

Experimental details

The cell fabrication process is suitable for both c-Si and mc-Si substrates. The commercial 156 mm × 156 mm p-type mc-Si with resistivity of 1–3 Ω cm and thickness of 200 ± 20 μm that we used in our experiment is from adjacent positions of a single silicon ingot. The processing sequence is shown in Fig. 1. After conventional cleaning and acidic texturization, the wafers underwent a 55 Ω sq^{-1} POCl$_3$ diffusion, then were
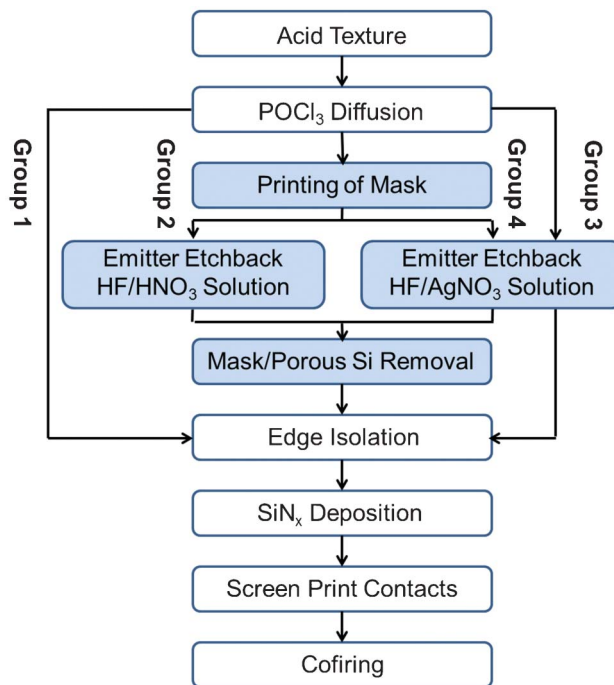

Fig. 1 Process flow diagram for the four groups of mc-Si solar cells. Group 1 is made by a standard mc-Si solar cell process, Group 2 by the standard etch-back SE process provided by SCHMID, Group 3 by an mc-Si nano-emitter solar cell process, and Group 4 by our mc-Si selective nano-emitter solar cell process.

divided into four groups. For comparison, Group 1 and Group 2 went through the standard solar cell process and an etch-back SE process provided by SCHMID. The wafers in Group 3 were soaked in a polytetrafluoroethene container with a mixture of 2.3 M HF and 0.01 M AgNO$_3$ at room temperature for 20 s and 40 s respectively to obtain nano-emitters. The silver contamination on the silicon surface was removed by HNO$_3$ in a sonication bath for 5 min. Then the following steps were in accordance with the standard process. The full fabrication flow of Group 4 was the same as that of Group 2 except for the etch-back process. The selective nano-emitters were fabricated by etching back the P diffused silicon wafers in a solution of 2.3 M HF and 0.01 M AgNO$_3$ for different lengths of time. The morphology and structures of the samples were characterized with a Hitachi S-4800 scanning electron microscope (SEM). Hemispheric total reflectance for normal incidence was measured on a Varian Cary 5000 spectrophotometer with an integrating sphere. The cell efficiency was measured by using a h.a.l.m. cetis PV-CT-L1. The EQE and IQE were measured by using PV Measurement System QEX7. The electroluminescence measurements (EL) were completed by BT Imaging LIS-R1.

Results and discussion

Fig. 2(a) shows an SEM image of p-type mc-Si with P diffusion on the front side after being immersed in AgNO$_3$/HF solution
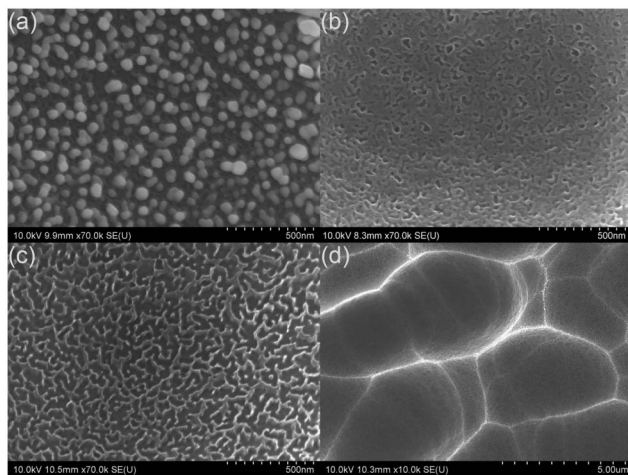
Fig. 2 (a) SEM image of P-diffused p-type mc-Si after being immersed in AgNO₃/HF solution for 20 s. (b) SEM image of nano-emitter which is etched back in AgNO₃/HF solution for 20 s with Ag removed. (c), (d) SEM images of nano-emitters after being etched back in AgNO₃/HF solution for 40 s with Ag removed.

Fig. 3 The effect of etching back time on sheet resistance (squares) and average reflectivity (spheres) in the wavelength range from 300 nm to 1000 nm.

for 20 s. As can be observed, silver nanoparticles with an average diameter of about 50 nm were embedded into the silicon surface. After removing the Ag nanoparticles by HNO_3, a shallow nanostructure layer appears on the silicon surface, as shown in Fig. 2(b). The mechanism of Ag-assisted chemical etching has been discussed in our previous works.[15,22] First of all, Ag^+ ions capture electrons from the silicon surface, deoxidize into Ag atoms, and then adhere to the silicon substrate. Simultaneously, the silicon underneath the Ag nuclei is oxidized into SiO_2 and then dissolved by HF. Owing to the higher electronegativity, Ag nuclei adhering to the silicon surface strongly attract electrons from Si to become negative, which has a strong catalytic influence on the cathodic reaction. Therefore, the nanostructure comes out. As the etching time increases, the depth of the nanostructure becomes deeper, as shown in Fig. 2(c). Fig. 2(d) is an SEM image of the silicon substrate after being etched for 40 s. It can be clearly seen that the overall morphology of the substrate is not changed much by the nanostructure layer.

However, the key of the etch-back process is to control the emitter sheet resistance. So the samples were soaked in AgNO₃/HF solution for different lengths of time ranging from 20 s to 60 s. Fig. 3 shows the sheet resistance and average reflectivity in the wavelength range from 300 nm to 1000 nm of the etched back silicon wafer as a function of etching time. The sheet resistance of the silicon wafer is 55 Ω sq⁻¹ after conventional POCl₃ diffusion, and then it increases from 67 Ω sq⁻¹ to 175 Ω sq⁻¹ when the etching time increases from 20 s to 60 s. The sheet resistance increases slowly at first and then more rapidly. Both the reaction rate and the homogeneity of the sheet resistance are well controlled. On the other hand, due to a gradually varying refractive index,[10] the nanostructure layer that forms on the silicon surface turns into an effective light trapping medium, which further reduces the reflectivity
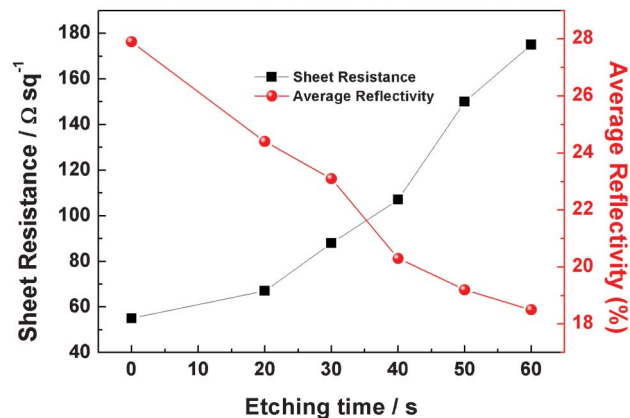
of the wafers. As the etching time increases, the color of the etched back silicon wafers is gradually deepened. The average reflectivity in the wavelength range from 300 nm to 1000 nm of the silicon wafer is 27.9% before the etch-back process and decreases to 24.4% after etching for 20 s. When the etching time increases to 60 s, the average reflectivity of the silicon wafer is further reduced to 18.5%. There is a very good correspondence between the average reflectivity and the wafers' appearance.

According to the discussion above, 20 s was chosen to etch back the emitters. After the etch-back process, standard processes are employed to finish the NE solar cell fabrication. The result measured by h.a.l.m. cetis PV-CT-L1 with calibrated 1-Sun simulators shows that the conversion efficiency (η) of the NE solar cell with a 67Ω sq⁻¹ sheet resistance (NE1) is 16.37%, with a 617 mV open-circuit voltage (V_{oc}), a 34.10 mA cm⁻² short current (J_{sc}) and a 77.8% fill factor (FF), as shown in Table 1. Compared to our previous black silicon solar cell which has a SiO_2/SiN_x double passivation layer, the four solar cells' main parameters are all improved. The increased V_{oc} implies a decrease of recombination in the solar cell, which is mainly attributed to the etch-back process. For our previous black silicon solar cell, the surface nanostructure was fabricated before POCl₃ diffusion, which worsens both the surface recombination and the Auger recombination.[16] On the nanostructured silicon surface, the diffused phosphorus

Table 1 Performance of different mc-Si solar cells

Sample	V_{oc} (mV)	J_{sc} (mA cm⁻²)	FF (%)	Effi. (%)
Black silicon solar cell[15]	604	33.89	77.3	15.82
Standard solar cell	617	34.00	78.1	16.38
Standard SE solar cell	619	34.64	77.4	16.60
NE solar cell (67 Ω sq⁻¹)	617	34.10	77.8	16.37
NE solar cell (107 Ω sq⁻¹)	610	33.69	76.9	15.80
SNE solar cell (89 Ω sq⁻¹)	619	34.08	78.3	16.52
SNE solar cell (107 Ω sq⁻¹)	624	35.16	77.2	16.94
SNE solar cell (151 Ω sq⁻¹)	626	35.02	76.7	16.81
SNE solar cell (175 Ω sq⁻¹)	620	34.86	77.2	16.68

dopant profile is significantly different from that on flat silicon for a given sheet resistance. Such increased Auger recombination results from the more heavily doped nano-emitter associated with the larger surface area and the lower dimensional scale of nanostructures. For a better under-standing of this issue, after conventional acid texturing, silicon wafers were etched in 2.3 M HF and 0.01 M $AgNO_3$ solution at room temperature for 0 s, 40 s, 50 s, 60 s, respectively, and then diffused with standard 75 Ω sq^{-1} and 80 Ω sq^{-1} POCl$_3$ diffusion process. As shown in Fig. 4, the sheet resistances of acid textured wafers are 75.1 Ω sq^{-1} and 79.8 Ω sq^{-1} after diffusion, which are very close to the standard values. However, nano-textured silicon wafers have lower sheet resistance than the acid textured ones. As the etching time and the size of the nanostructure increases, the sheet resistance decreases, implying that nanostructure has a heavier doping level on the surface. The relationship between Auger lifetime and concentration of both majority carriers and minority carriers for an n-type emitter is:[23]

$$\tau_{Aug} = \frac{1}{Cnp + Dn^2} \quad (1)$$

where τ_{Aug} is Auger lifetime; n is the concentration of free electrons; p is the concentration of free holes; C is a constant depending on the material; and D is the Auger coefficient based on the material. Auger recombination rate is propor-tional to the square of the P dopant concentration. The increased doping level of the nano-textured black silicon solar cell certainly worsens the Auger recombination, which finally leads to a drop in the solar cell's efficiency. As to the NE solar cells, the etch-back process is carried out after the emitter formation. In this case, the danger of heavy doping caused by the nanostructure will not happen. Furthermore, there is usually a dead layer in the vicinity of the silicon surface after conventional P diffusion. As the etch-back process proceeds,

the dead layer is removed, resulting in the decrease of Auger recombination.

As we mentioned before, the reduced conversion efficiency of the solar cell is mainly attributable to optical losses and electrical losses. The lower reflectivity alone does not ensure a higher short current. As shown in Fig. 5, the average reflectivity of a black silicon solar cell in the wavelength range from 300 nm to 1000 nm is 9.82%, while that of the NE solar cell with a 67 Ω sq^{-1} sheet resistance is 11.01%. Although more reflective, the J_{sc} of NE1 is better than the black silicon solar cell. Such increased J_{sc} can be attributed to the improved ohmic contact, and the decreased Auger recombination which is related to reduced sheet resistance. As we found previously, the electrode contact is quite poor between the black silicon surface and the screen-printed Ag-based front grid due to the reduced contact area between the nanostructures and the Ag metal.[15] However, the nanostructures in NE1 are rather thin, so it is unsurprising that it has good contact with the Ag-based front grid. At the same time, the fill factor is also enhanced by the improved electrode contact.

When compared with the conventional solar cells (Group 1), a slight increase in the short current of the NE1 solar cells can be attributed to the enhanced light trapping and decreased Auger recombination. However, the conversion efficiency has no significant enhancement, which results from the non-optimized passivation. The passivation provided by a single SiN$_x$ layer cannot completely passivate the nanostruc-ture, according to our previous findings.

As discussed above, the reflectivity of NE1 has just a slight decrease. In order to further increase the light absorption and suppress the Auger recombination, the etch-back time is prolonged to 40 s and the sheet resistance is increased to 107 Ω sq^{-1}. However, the performance of the NE solar cell with a 107 Ω sq^{-1} sheet resistance (NE2) turns out to be bad. Such a decline can be mainly attributed to the terrible contact in the
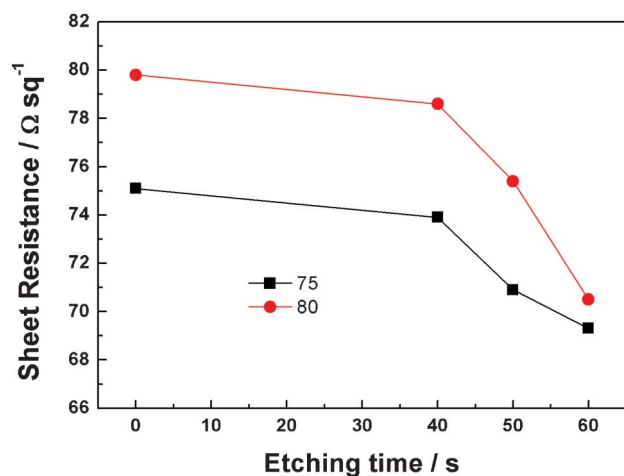
Fig. 4 The sheet resistance of the nanostructure etched for different lengths of time after being diffused with standard 75 Ω sq^{-1} (squares) and 80 Ω sq^{-1} (spheres) POCl$_3$ diffusion processes.
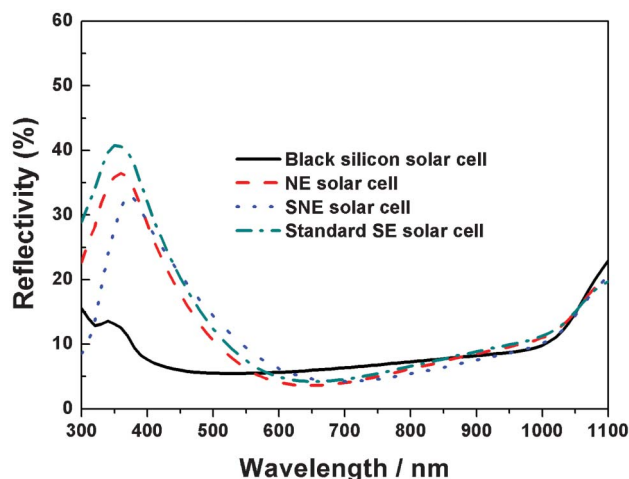
Fig. 5 Total hemispherical reflectance of black mc-Si solar cell, mc-Si nano-emitter solar cell with a 67 Ω sq^{-1} sheet resistance, mc-Si selective nano-emitter solar cell with a 107 Ω sq^{-1} sheet resistance, and standard mc-Si etch-back SE solar cell.

metal/semiconductor interface as a result of a high sheet resistance. The carrier collection is another important issue in the solar cells, which can greatly influence the conversion efficiency. Therefore, the etch-back time of an NE solar cell should not be too long in order to obtain good ohmic contact. Failing this, the benefits of the nano-emitter will not be adequately achieved.

With the purpose of fully realizing the potential advantages of our nano-emitter, a selective emitter process was combined with our etch-back technique, producing a selective nano-emitter (SNE). In the SE technique, the contact region is masked with wax by inkjet printing before the etch-back process. The emitter underneath the contact therefore is protected by such acid resistant material and not etched by the HF/AgNO$_3$ solution. In this case, nanostructure will not be formed in the contact region, which ensures a good ohmic contact. On the other hand, the etch-back time can be longer to achieve lower reflectivity and higher sheet resistance in the illuminated region. In order to get a good point, the etching back time varies from 30 s to 60 s with a time interval of 10 s. As a result, the sheet resistance of the illuminated region is 89 Ω sq^{-1}, 107 Ω sq^{-1}, 151 Ω sq^{-1}, 175 Ω sq^{-1}, respectively (Fig. 3). The measurements of the SNE solar cells are compared to those of conventional cells in Table 1. As can be observed, with the SE technique, the conversion efficiency of SNE solar cells is significantly better than that of NE solar cells. Both open-circuit voltage and short current have been enhanced by various degrees. As mentioned above, with the etching back time prolonged, the sheet resistance and light absorption of solar cell increases. The further suppression of Auger recombination related to the higher sheet resistance enhances both the V_{oc} and J_{sc}. The improved light absorption and electrode contact also increase the short current. When the SNE solar cells are investigated in detail, it is found that with an increase of sheet resistance, both V_{oc} and J_{sc} increase at first and then decrease. Open-circuit voltage is improved at the beginning as a result of the increased sheet resistance and the inhibited Auger recombination. As the sheet resistance increases further – exceeding 151 Ω sq^{-1} – it cannot form an effective potential difference, resulting in a decrease in V_{oc}. Short current increases at first because of the reduced reflectivity and Auger recombination, and then it declines due to the aggravated surface recombination associated with the deepened nanostructure. The best SNE solar cell is the one with 107 Ω sq^{-1} sheet resistance whose conversion efficiency is 16.94%, accomplished by balancing sheet resistance, reflectivity, potential difference and surface recombination.

In comparison with the standard SE solar cells in Group 2, the efficiency of the SNE solar cells in Group 4, except the one with 89 Ω sq^{-1} sheet resistance, is significantly raised by employing the HF/AgNO$_3$ mixture as etch-back solution instead of the HF/HNO$_3$ system (Table 1). The sheet resistance of the standard selective emitter in Group 2 is around 100 Ω sq^{-1}. The increase of V_{oc} can be attributed to a higher sheet resistance and a more uniform emitter. The suppressed Auger recombination and the increased light absorption together

lead to a higher J_{sc}. For a standard SE solar cell, a porous silicon layer is formed during the etch-back process and then removed by NaOH solution since it is hard to passivate. However, such an etch-back process results in variations of the texturing morphology, which increase the reflectivity.[24] In contrast, the reflection of SNEs is reduced thanks to the gradually varying refractive index of the nanostructure layer. As shown in Fig. 5, the average reflectivity of the best SNE solar cell and the standard SE solar cell is 10.15% and 11.31% respectively in the wavelength range from 300 nm to 1000 nm. With the nanostructured etch-back layer, the suppression of reflection is mainly for the shortest wavelength light, which enhances the blue response.[13] According to the discussion above, SNE etched back by HF/AgNO$_3$ solution can be a potential substitute of standard etch-back SE because of a lower reflectivity and a more homogeneous emitter related with a more controllable process.

Fig. 6 shows the internal quantum efficiency (IQE) and external quantum efficiency (EQE) of the black silicon solar cell and the solar cells in four different groups. As can be observed, although the black silicon solar cell has the highest absorption in the wavelength range from 300 nm to 550 nm, the EQE in this region is the lowest of these five kinds of solar cells, as well as the IQE. Such low IQE, arising from both high Auger recombination and surface recombination, eliminates the advantage of low reflectance. When the nano-emitter is fabricated after POCl$_3$ diffusion (NE), both EQE and IQE are improved in the wavelength range from 300 nm to 550 nm thanks to the reduced recombination. Compared to standard mc-Si solar cells (Group 1), nano-emitter solar cells have a lower IQE, as a result of the nanostructure-related surface recombination, from 300 nm to 400 nm, but a higher EQE at the wavelength range from 300 nm to 350 nm, benefiting from lower reflectivity. The selective nano-emitter solar cell with a sheet resistance of 107 Ω sq^{-1} (Group 4) has the best blue response of all. Both EQE and IQE are higher than standard SE solar cells (Group 3) due to the reduced reflectivity and Auger recombination, and it is a more uniform emitter as well.

Electroluminescence measurements were made in order to investigate the details of standard mc-Si SE solar cell and the best mc-Si SNE solar cell, as shown in Fig. 7. The dark regions in the EL image are related to low minority carrier lifetime, associated with high series resistance caused by nonuniform resistance. As can be observed, such dark regions are more visible in the standard mc-Si SE solar cell than in the mc-Si SNE solar cell, which indicates that the nano-emitter etched back by HF/AgNO$_3$ solution has a more homogeneous sheet resistance than is obtained with the standard etch-back process.

Conclusion

In conclusion, a nano-emitter has successfully fabricated by one-step Ag-assisted chemical etch-back after conventional p-n junction formation. Compared with our previous black silicon,
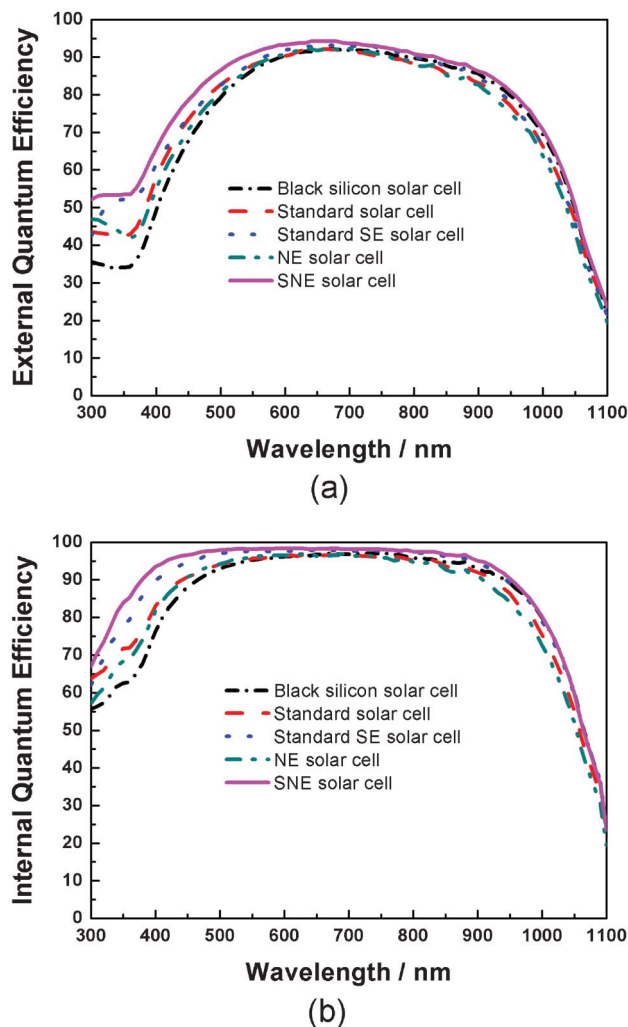
Fig. 6 Comparison of external quantum efficiency (a) and internal quantum efficiency (b) of black mc-Si solar cell, standard mc-Si solar cell, standard mc-Si etch-back SE solar cell, mc-Si nano-emitter solar cell with a 67 Ω sq⁻¹ sheet resistance, and mc-Si selective nano-emitter solar cell with a 107 Ω sq⁻¹ sheet resistance.

whose nano-emitter is formed before $POCl_3$ diffusion, the conversion efficiency of the NE solar cell that was etched back in $HF/AgNO_3$ solution for 20 s is significantly better, thanks to
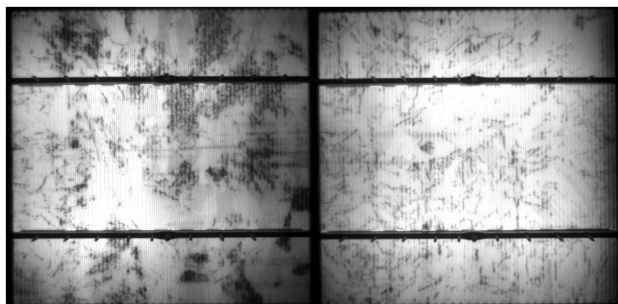
Fig. 7 Electroluminescence (EL) image of standard mc-Si SE solar cell (left) and the best mc-Si selective nano-emitter solar cell (right).

an increased open-circuit voltage, short current and fill factor. The reduced surface recombination and Auger recombination that result from the etch-back process lead to an increase in V_{oc}. In spite of higher reflectivity, however, the J_{sc} increases due to the improved ohmic contact, and decreased Auger recombination which is related to reduced sheet resistance. However, as the etch-back time increases, the performance of the NE2 drops, due to the bad contact in the metal/semiconductor interface, associated with the high sheet resistance. In order to further increase the light harvest and suppress Auger recombination, the nano-emitter solar cell is modified by a selective emitter technique, resulting in our mc-Si selective nano-emitter solar cell. By varying the sheet resistance of the emitter from 89 Ω sq⁻¹ to 175 Ω sq⁻¹, a 16.94% conversion efficiency is finally achieved with a 107 Ω sq⁻¹ sheet resistance, which is higher than the standard SE solar cell's efficiency of 16.60%. Such improved efficiency can be attributed to the reduced reflectivity and a more homogeneous emitter when employing $HF/AgNO_3$ solution as the etch-back system instead of the HF/HNO_3 mixture. The selective nano-emitter solar cell really represents some progress beyond black silicon solar cells; however, the advantage of low reflectivity is not fully achieved. An innovative solution, which avoids the increase of both surface and Auger recombination, should be found to achieve a real low-reflection black silicon solar cell.

Acknowledgements

References

1 P. Campbell and M. A. Green, *J. Appl. Phys.*, 1987, **62**, 243.
2 R. Einhaus, E. Vazsonyi, J. Szlufcik, J. Nijs and R. Mertens, *Conference Record of the Twenty Sixth IEEE Photovoltaic Specialists Conference - 1997*, 1997, 167.
3 K. Q. Peng and S. T. Lee, *Adv. Mater.*, 2011, **23**, 198.
4 H. C. Yuan, V. E. Yost, M. R. Page, P. Stradins, D. L. Meier and H. M. Branz, *Appl. Phys. Lett.*, 2009, **95**, 123501.
5 E. V. Kerschaver and G. Beaucarne, *Progr. Photovolt.: Res. Appl.*, 2006, **14**, 107.
6 T. H. Her, R. J. Finlay, C. Wu, S. Deliwala and E. Mazur, *Appl. Phys. Lett.*, 1998, **73**, 1673.
7 H. Jansen, M. D. Boer, R. Legtenberg and M. Elwenspoek, *J. Micromech. Microeng.*, 1995, **5**, 115.
8 K. Q. Peng, J. J. Hu, Y. J. Yan, Y. Wu, H. Fang, Y. Xu, S. T. Lee and J. Zhu, *Adv. Funct. Mater.*, 2006, **16**, 387.
9 C. C. Striemer and P. M. Fauchet, *Appl. Phys. Lett.*, 2002, **81**, 2980.
10 L. L. Ma, Y. C. Zhou, N. Jiang, X. Lu, J. Shao, W. Lu, J. Ge, X. M. Ding and X. Y. Hou, *Appl. Phys. Lett.*, 2006, **88**, 171907.

11 H. Jansen, M. D. Boer, R. Legtenberg and M. Elwenspoek, *J. Micromech. Microeng.*, 1995, **5**, 115.

12 R. Dussart, X. Mellhaoui, T. Tillocher, P. Lefaucheux, M. Volatier, C. S. Clerc, P. Brault and P. Ranson, *J. Phys. D: Appl. Phys.*, 2005, **38**, 3395.

13 H. M. Branz, V. E. Yost, S. Ward, K. M. Jones, B. To and P. Stradins, *Appl. Phys. Lett.*, 2009, **94**, 231121.

14 Z. P. Huang, N. Geyer, P. Werner, J. D. Boor and U. Gösele, *Adv. Mater.*, 2011, **23**, 285.

15 Y. P. Liu, T. Lai, H. L. Li, Y. Wang, Z. X. Mei, H. L. Liang, Z. L. Li, F. M. Zhang, W. J. Wang, A. Y. Kuznetsov and X. L. Du, *Small*, 2012, **8**, 1392.

16 J. Oh, H. C. Yuan and H. M. Branz, *Nat. Nanotechnol.*, 2012, **7**, 743.

17 M. J. Kerr, J. Schmidt, A. Cuevas and J. H. Bultman, *J. Appl. Phys.*, 2001, **89**, 3821.

18 M. Gauthier, M. Grau, O. Nichiporuk, F. Madon, V. Mong-The Yen, N. Le Quang, A. Zerga, A. Slaoui, D. Blanc-Pélissier, A. Kaminski-Cachopo and M. Lemiti, *24th European Photovoltaic Solar Energy Conference*, 21–25 September 2009, Hamburg, Germany, p. 1875.

19 H. Antoniadis, F. Jiang, W. Shan and Y. Liu, *Proceedings of the 35th IEEE Photovoltaic Specialists Conference*, 2010, 1193.

20 A. Dastgheib-Shirazi, H. Haverkamp, B. Raabe, F. Book and G. Hahn, *Proceedings of the 23th European photovoltaic solar Energy conference*, Valencia,Spain, 1–5 September 2008.

21 B. Tjahjono, H. Haverkamp, V. Wu, H. T. Anditsch, W.-H. Jung, J. Cheng, J. Ting, M. J. Yang, D. Habermann, T. Sziptalak, C. Buchner, C. Schmid, B. Beilby and K.-C. Hsu, *26th European Photovoltaic Solar Energy Conference and Exhibition, 2AO.3.6*, 2011, 901.

22 Y. Wang, Y. P. Liu, H. L. Liang, Z. X. Mei and X. L. Du, *Phys. Chem. Chem. Phys.*, 2013, **15**, 2345.

23 J. I. Pankove, *Optical Processes in Semiconductors[M]*, Englewood Cliffs, N. J., Prentice-Hell, 1971.

24 Z. C. Liang, F. Zeng, H. Song and H. Shen, *Sol. Energy Mater. Sol. Cells*, 2013, **109**, 26.